$$dA'_Z(r') = (\mu_0/4\pi)I(z')\exp(-jkr')dz' \quad \text{(A2)}$$

Performing the curl operation on Eq. (A2) in spherical coordinates then gives Eq. (1). Maxwell's curl-H equation then gives Eqs. (2) and (3).

APPENDIX B: INTEGRAL EXPRESSION FOR $e_r(r/h, \theta)$

Following the same procedure as that to obtain

$$e_\theta(r/h, \theta)$$

upon using (15) through (18) into:

$$dE_r = \cos\theta\, dE_z + \sin\theta\, dE_y \quad \text{(B1)}$$

gives

$$dE_r = \cos(\theta - \theta')dE'_r + \sin(\theta - \theta')dE'_\theta \quad \text{(B2)}$$

Using Eqs. (2) and (3) in Eq. (B2) and normalizing gives

$$e_r(r/h, \theta) = 0.50\left(\frac{a}{h}\int_{-1/2}^{1/2}[\{C + j(DQ - CQ^{-1})\}(r/h)^{-2}\right)^{\exp(-jQ)dw} \quad \text{(B3)}$$

where

$$C = 2\cos\theta'\cos(\theta - \theta') + \sin\theta'\sin(\theta - \theta') \quad \text{(B4)}$$

$$D = \sin\theta'\sin(\theta - \theta') \quad \text{(B5)}$$

REFERENCES

1. H. Hertz, Electric waves, Macmillan, New York, 1893; translated by D.E. Jones.
2. J.A. Barth, Collected works of H. Hertz, Vol. 2, 3rd ed., Leipzig, 1914, p. 147.
3. J.A. Stratton, Electromagnetic theory, McGraw-Hill, New York, 1941, pp. 434–437.
4. A.B. Bronwell and R.E. Beam, Theory and application of microwaves, McGraw-Hill, New York, 1947, pp. 402–407.
5. W.R. Smythe, Static and dynamic electricity, 2nd ed., McGraw-Hill, New York, 1950, pp. 469–472.
6. E.C. Jordan, Electromagnetic waves and radiating systems, Prentice Hall, New York, 1950, pp. 303–309.
7. H.P. Williams, Antenna theory and design, Vol. 1, Sir Isaac Pitman and Sons, London, 1950, pp. 64–70.
8. W.K.H. Panofsky and M. Phillips, Classical electricity and magnetism, Addison-Wesley, Cambridge, MA, 1955, pp. 222–225.
9. S. Silver, Microwave antenna theory and design, Boston Technical Publishers, Lexington, MA, 1964, pp. 92–95; originally published as Vol. 12, MIT Rad. Lab. Series, McGraw-Hill, New York, 1947, pp. 92–95.
10. A. Sommerfeld, Electrodynamics, Academic Press, New York, 1952, pp. 148–152.
11. E.C. Jordan and K. Balmain, Electromagnetic waves and radiating systems, 2nd ed., Prentice Hall, New York, 1968, p. 317–323.
12. R.E. Collin and F.J. Zucker, Antenna theory, Part I, McGraw-Hill, New York, 1969, pp. 29–32.
13. A.W. Rudge, K. Milne, A.D. Olver, and P. Knight, The handbook of antenna design, Vol. 1, Peter Pregrinus, London, 1982, pp. 49–52.
14. J. Van Bladel, Electromagnetic fields, Hemisphere Publishing, New York, 1985, pp. 216–217.
15. Y.T. Lo and S.W. Lee, Antenna handbook, Van Nostrand, New York, 1988, pp. 3–13.
16. E.A. Wolff, Antenna analysis, Artech House, Norwood, MA, 1988, pp. 24–27.
17. S. Ramo, J.R. Whinnery, and T. Van Duzer, Fields and waves in communication electronics, 3rd ed., Wiley, New York, 1994, pp. 589–592.
18. J.A. Kong, Electromagnetic wave theory, 2nd ed., Wiley, New York, 1990, pp. 235–240.
19. R.C. Johnson, Antenna engineering handbook, 3rd ed., McGraw-Hill, New York, 1993, p. 2; also edition 2, R.C. Johnson and H. Jasik (1984), and Edition 1, H. Jasik, 1961, p. 2.
20. W.L. Stuzman and G.A. Thiele, Antenna theory and design, 2nd ed., Wiley, New York, 1998, p. 21; also first edition (1981), p. 14.
21. J.L. Volakis, Antenna engineering handbook, 4th ed., McGraw-Hill, New York, 2007, pp. 1–7 and 1–8.
22. R.W.P. King, The theory of linear antennas, Cambridge, MA, Harvard University Press, 1956, pp. 698–700.
23. M. Abraham and R. Becker, The classical theory of electricity and magnetism, 2nd English ed., Hafner Publishing, New York, 1949, p. 224.
24. Reference data for radio engineers, Federal Telephone and Radio, New York, 1949, p. 364.
25. H.H. Skilling, Fundamentals of electric waves, Wiley, New York, 1949, p. 165.
26. J.D. Kraus, Antennas, 2nd ed., McGraw-Hill, New York, 1950, p. 128, 1988, p. 203.
27. S.A. Schelkunoff and H.T. Friis, Antennas theory and practice, Wiley, New York, 1952, p. 120.
28. J.R. Wait, Electromagnetic radiation from cylindrical structures, Pergamon Press, New York, 1959, pp. 170–171.
29. H.W. Sams, Reference data for radio engineers, 5th ed., H.W. Sams, New York, 1968, p. 25–31.
30. C.A. Balanis, Antenna theory—Analysis and design, Harper and Row, New York, 1982, p. 103.
31. B.I. Bleaney and B. Bleany, Electricity and magnetism, Vols. 1 and 2 (Two volume edition), Oxford University Press, Oxford, UK, 1989, p. 251.
32. C.A. Balanis, Antenna theory—Analysis and design, 2nd ed., Wiley, New York, 1997, p. 136.
33. J.D. Kraus and R.J. Marhefka, Antennas for all applications, 3rd ed., New Delhi, 2003, p. 168.
34. C.A. Balanis, Antenna theory and design–Analysis and experiment, 3rd ed., Wiley, New York, 2005, p. 154.
35. F.E. Terman, Radio engineering handbook, McGraw-Hill, New York, 1944, p. 773.
36. S.A. Schelkunoff and H.T. Friis, Antennas theory and practice, Wiley, New York, 1952, p. 342.
37. C.M. Knop and R. Frazer, A study of small-height HF jamming antennas for vehicular use, Microwave Opt Technol Lett 13 (1996), pp. 267–274.
38. C.A. Balanis, Antenna theory—Analysis and design, Harper and Row, New York, 2005, p. 151.
39. R.C. Hansen, Electrically small, super directive, and superconducting antennas, Wiley, New Jersey, 2006, pp. 17–25; pp. 55–57.

© 2012 Wiley Periodicals, Inc.

A TRI-BAND, SMALL SIZE RADIO FREQUENCY IDENTIFICATION TAG ANTENNA WITH U-SHAPED SLOTS

Hanieh Aliakbari,[1] Alireza Mallahzadeh,[2] and Sajad Mohammad Ali Nezhad[3]
[1] Department of Electrical Engineering, Amirkabir University of Technology, Tehran, Islamic Republic of Iran; Corresponding author: H.Aliakbari@aut.ac.ir
[2] Department of Electrical Engineering, Faculty of Engineering, Shahed University, Tehran, Islamic Republic of Iran
[3] Department of Electrical Engineering, Faculty of Engineering, Shahed University, Tehran, Islamic Republic of Iran

Received 29 September 2011

ABSTRACT: *A new multiband, small size antenna for passive radio frequency identification (RFID) tags is presented. Placement of three U-shaped slots can create three independent resonances within the RFID range: 0.953, 2.45, and 5.8 GHz, whereas in each resonance, particular inductive input impedance will be achieved by a simple*

technique to be conjugately matched with the capacitive impedance of the chosen electronic chip. The proposed simple structural antenna is flexibly tunable to be matched with other chips in RFID frequencies. It is shown that the matching and forward patterns of tag antenna in each band are desirable, simultaneously. Details of the proposed antenna design and measured results are presented. © 2012 Wiley Periodicals, Inc. Microwave Opt Technol Lett 54:1975–1978, 2012; View this article online at wileyonlinelibrary.com. DOI 10.1002/mop.26949

Key words: *triband; RF identification; tag; slot antenna*

1. INTRODUCTION

Radio frequency identification (RFID) is a technology used for objects automatic identification. The antenna is a major component in the layout of passive RFID tags and plays an important role in determining the overall performance of RFID systems. It is usually desirable to have a small RFID tag printed on a single substrate with inductive input reactance to be conjugately matched with the capacitive reactance of the passive RFID integrated circuit in RFID frequencies. RFID systems that cover the frequency bands of microwave band range 860–960 MHz, 2.45 GHz, and 5.8 GHz has the advantage of longer reading range with a higher data transfer rate in comparison with the RFID systems, which use lower frequencies. Conversely, because RFID tags need to be attached on various objects with different shapes and material properties to design an antenna prototype which minimizes the variations of input impedance, use of ground plane is suggested in Ref. 1. Various techniques have been applied for conjugate matching between chip and tag antenna. For example, in Ref. 2, parasitic element produces the equivalent inductive impedance, Moreover, using open stub feed in Ref. 3 and also adding T-match Network in Ref. 4 have been reported. Among the wide variety of RFID applications, the design of multiband tag antennas is very attractive. Various dual-band antennas have been designed for RFID communications, which combine the UHF and microwaves frequency (2.45 GHz). The self-similarity nature of fractal for designing dual-band tag antenna has been reported in Refs. 4 and 5, the dual-band concept is applied to the design of impedance-matching networks, in which its synthesis is based on a perturbation method. Nevertheless, those RFID tags need not only good impedance matching to attain efficient power transfer between the antenna and the tag chip but also a compact size to be flexibly integrated within different modern portable devices, for example, in Ref. 6 author uses the space-filling nature of dual-band meander line antenna for size reducing. However, so far, reported tags feeding with RFID chips are only focused on single- and dual-band antennas, because matching in more than two frequencies, with almost high-input capacitive impedance of chip, is very difficult. In such works, authors have designed tag structures that are too complex and almost untunable thus when the chip is upgraded to a new version, the RFID tag designers must redesign the tag, which is obviously undesirable. Finally, considering all above necessities along with size reducing is very difficult.

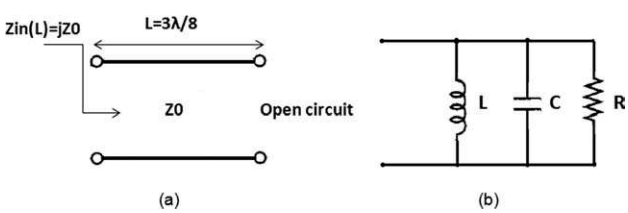

Figure 1 (a) Equivalent stub model for U-shaped slot and (b) equivalent circuit model of the proposed tag antenna

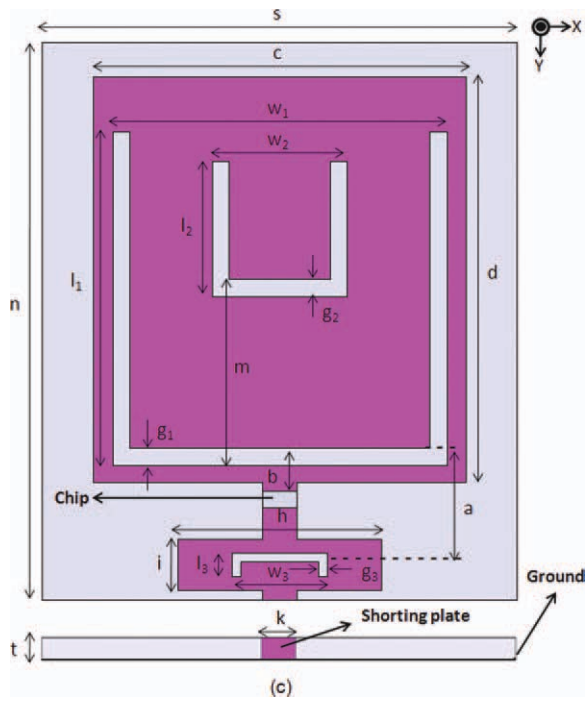

Figure 2 Geometry of proposed RFID tag antenna (Top and opposite view). Design parameters are: S= 28 mm, n= 33 mm, t= 0.8 mm, c= 22 mm, d = 24 mm, w_1 = $l1$ = 19.74 mm, $g1$ = $g2$ = 1 mm, g_3 = 0.5 mm, m = 11 mm, $w2$ = $l2$ = 8 mm, a = 6.7 mm, $l3$ = 1.4 mm, $w3$ = 5.6 mm, h = 12 mm, i = 3 mm, k = 2 mm, b = 2.5 mm. [Color figure can be viewed in the online issue, which is available at wileyonlinelibrary.com]

In this letter, a novel tri-band, small size tag antenna suitable for RFID application is presented. The proposed tunable tag antenna has good matching in three RFID bands: 0.953, 2.4, and 5.8 GHz, simultaneously. The forward patterns in center frequencies are also desirable. Details of antenna design are presented. Simulation results via software package HFSS and measured results are given.

2. ANTENNA STRUCTURE AND DESIGN

As indicated, to achieve the goal of conjugate matching between the capacitive impedance of chip and tag antenna, we need to establish a particular value of input reactance. Placement of U-shaped slot in the rectangular patch can create equivalent inductive circuit and be modeled as the open-circuit stub [Fig. 1(a)]. The antenna, fabricated on a 3.3 × 2.8 × 0.8 cm^3, FR4 substrate with dielectric constant ε_r = 4.4 and loss tangent tanδ = 0.02 consist of three U-shaped slots with the total length of $(3\lambda_g)/8$

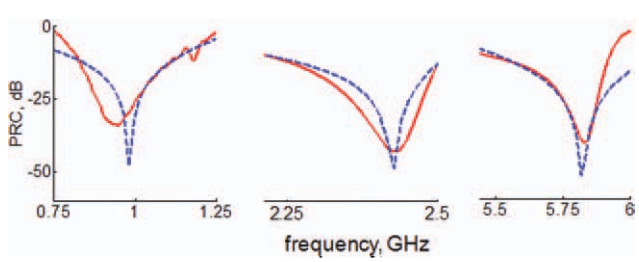

Figure 3 Measured and simulated return loss. – – – – Simulated; ——— measured. [Color figure can be viewed in the online issue, which is available at wileyonlinelibrary.com]

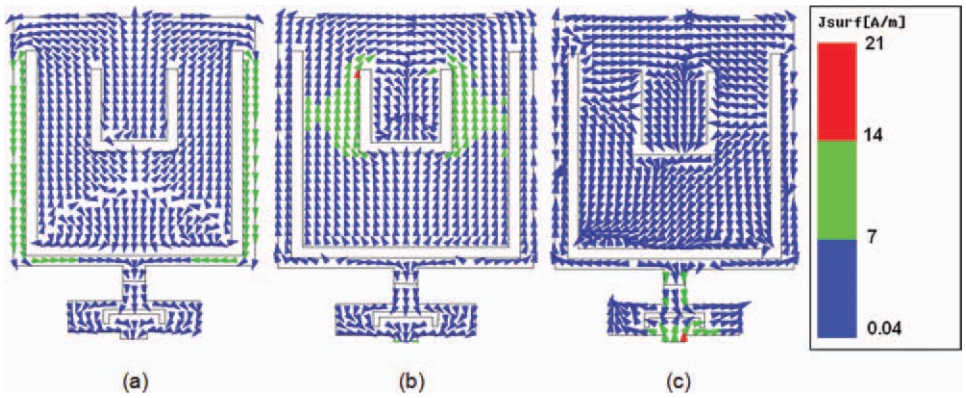

Figure 4 Current distribution of tri-band tag antenna at: (a) 953 MHz, (b) 2.45 GHz, and (c) 5.8 GHz. [Color figure can be viewed in the online issue, which is available at wileyonlinelibrary.com]

on one side of a dielectric substrate, each related to one RFID frequency and also a large metal ground is placed on the opposite side, which make the proposed antenna mountable on metallic surfaces. These slots can be served as a resonator, because in the air regions of the slot, the magnetic field lines make curve and return to the slot region at 3/8 the guided wavelength interval. It is found that by varying the total length of the U-shaped slots, the resonant frequency of the tag can be adjusted easily, which in this case cover 0.953, 2.45, and 5.8 GHz. As indicated in Figure 1(a), the input reactance is related to the characteristic impedance of the stub. Under the fixed dimension of total length, variation of $g_i s$ (i=1, 2, 3) will tune the impedance of the equivalent open-circuit stub model, resulting in tuning the reactance value of the tag antenna. The energy transmission between chip and patch is achieved by microstrip feed which allows for having multiband structure. The distance between chip and slot in addition to the direction of the slot, with respect to the chip, will tune the resistance of the antenna's inductive impedance at related RFID frequency to achieve conjugate match with the various values of the chip impedances in RFID frequencies. Consequently, the resulting equivalent circuit model of the proposed tag antenna is illustrated in Figure 1(b).

This simple technique will create independent bands and also tune input impedance of these antennas, flexibly in large scale with various lengths and different positions of U-shaped slot for different RFID chips. The whole geometry with detailed design parameters of the proposed small size, tri-band tag antenna is shown in Figure 2. The antenna is easy to be fabricated because the symmetric structure requires no through holes connecting to the metal ground and also could be tuned to be matched with other different RFID chips at different RFID frequencies. In this study, by tuning the dimensions, the impedance of the tag antenna could be the complex conjugate of the chip, which has input impedance as follows: (10−56j) Ω at f = 953 MHz, (10−22j) Ω at f = 2.45 GHz, and (10−9.3j) Ω at f=5.8 GHz also the antenna size has been reduced to a small volume, to be easily integrated within various portable devices.

By optimizing the proposed structure parameters, the structure resonates at three different RFID frequencies with the desired inductive input impedances, simultaneously.

3. SIMULATED AND EXPERIMENTAL RESULTS

On the basis of Kurokawa method, the following useful return loss definition is introduced for cases that the circuit is connected to the complex source [4]:

$$\text{Return loss} = \left|\frac{Z_L - Z_C^*}{Z_L + Z_C^*}\right|$$

Z_L is related to the antenna impedance and Z_C is the chip impedance. The simulated and measured return loss in Figure 3 demonstrate good matching between chip and tag antenna in three RFID frequencies. Current distributions (Fig. 4) show the dependent behavior of antenna in each resonant frequency, in which the maximum current density is around the corresponding U-shaped slot. The antenna has a favorable radiation pattern at center frequencies, and the antenna radiation patterns in xy and xz planes are illustrated in Figure 5. A unidirectional radiation patterns are obtained as the radiator is mounted on a vertical printed rectangular ground and maximum values appear in the forward direction (z-direction), whereas the peak gain is around 1.45, 3.1, and 2.4 dBi, respectively, at center frequencies. Acceptable agreement between measurement and simulation is observed.

4. CONCLUSIONS

A tri-band, small size RFID tag antenna with three U-shaped slot, on a 3.3 × 2.8 × 0.8 cm^3 substrate, covering RFID frequencies: 0.953, 2.45, and 5.8 GHz, is proposed. This simple

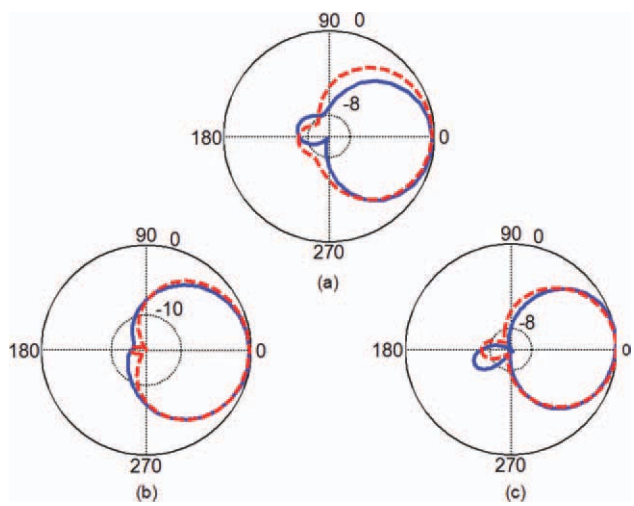

Figure 5 Radiation patterns of proposed antenna at three frequencies: – – – – yz plane; ——— xz plane; 953 MHz, (b) 2.45 GHz, and (c) 5.8 GHz. [Color figure can be viewed in the online issue, which is available at wileyonlinelibrary.com]

structure provides freedom to adjust the input inductive impedance to be conjugately matched with chosen RFID chips in different RFID frequencies. This tag antenna which is mountable on the metallic surface presents good matching in each of three independent bands, simultaneously, and also unidirectional radiation pattern at center frequencies with a maximum gain of about 1.45, 3.1, and 2.4 dBi, respectively, at center frequencies.

REFERENCES

1. L. Mo, H. Zhang, and H. Zhou, Broadband UHF RFID tag antenna with a pair of U slots mountable on metallic objects, Electron Lett 44 (2008), 1173–1174.
2. Y.-T. Im, J.-H. Kim, and W.-S. Park, Matching techniques for miniaturized UHF RFID loop antennas, IEEE Lett Antennas Propag 8 (2009), 266–270.
3. L. Mo and C. Qin, Planar UHF RFID tag antenna with open stub feed for metallic objects, IEEE Trans Antennas Propag 58 (2010), 3037–3043.
4. H. Kimouche, H. Zemmour, and B. Atrouz, Dual-band fractal shape antenna design for RFID applications, Electron Lett 45(2009), 1061–1063.
5. F. Paredes, G.Z. Gonzàlez, J. Bonache, F. Martín, Dual-band impedance-matching networks based on split-ring resonators for applications in RF identification (RFID), IEEE Trans Microwave Theory Tech 58 (2010), 1159–1166.
6. J.-Y. Park and J.-M. Woo, Miniaturized dual-band S-shaped RFID tag antenna mountable on metallic surface, Electron Lett 44 (2008), 1339–1341.

© 2012 Wiley Periodicals, Inc.

80–110 GHz MMIC AMPLIFIERS USING A 0.1-μm GaAs-BASED mHEMT TECHNOLOGY

Dong Min Kang and Hyung Sup Yoon
RF Convergence Components Research Team, Electronics and Telecommunications Research Institute, 161 Gajeong-Dong, Yuseong-Gu, Daejeon 305-350, Korea; Corresponding author: kdm1597@etri.re.kr

Received 30 September 2011

ABSTRACT: *A 80–110 GHz broadband MMIC low noise amplifiers (LNAs) have been developed for W-band passive image sensors. A monolithic microwave integrated circuit (MMIC) LNAs consists of a four-stage single-ended type and a four-stage balanced type. The chip set was fabricated using a 0.1-μm gate-length InGaAs/InAlAs/GaAs metamorphic high electron mobility transistor process based on a four-inch substrate. The single-ended type LNA (ver.1) achieved a gain of 20 dB over in a band between 85 and 105 GHz and a noise figure of lower than 5.3 dB in a frequency range of 86.5–100 GHz. The single-ended type LNA (ver.2) exhibited a gain of 27 dB with a noise figure of 4.3 dB at 94 GHz. The external DC biasing conditions of V_{ds} and V_{gs} were 1 and −0.2 V, respectively, and the total current consumption of the LNA was 40 mA. The chip size was 2 × 1.2 mm^2. The balanced-type amplifier demonstrated a measured small signal gain of over 18 dB from 80 to 100 GHz. The external DC biasing conditions of V_{ds} and V_{gs} were 1 and −0.2 V, respectively, and the total current consumption was 82 mA. The chip size was 2.9 × 2.5 mm^2.* © 2012 Wiley Periodicals, Inc. Microwave Opt Technol Lett 54:1978–1982, 2012; View this article online at wileyonlinelibrary.com. DOI 10.1002/mop.26948

Key words: *W-band; GaAs; mHEMT; MMIC; LNA*

1. INTRODUCTION

The passive millimeterwave (PMMW) image sensor is the image sensor, which senses the millimeter wave among the black-body radiation (black body radiation) generated in all objects. It uses frequency band such as 35, 94, 140, and 220 GHz in which the loss is less among the atmospheric.

As the millimeter wave, unlike the visible light and the IR, has a transparency about an object and sense the particular image, it is expected comprising the next generation image sense in which various applications are used.

Up-to-date, the PMMW image sensor mainly uses the optical lens, which sense the weak millimeter wave signal emitted in the black-body radiation and makes images. The main component of PMMW is W-band low noise amplifier (LNA), which amplifies the millimeter signal from objects, so it is required to develop LNA having high gain and low noise characteristics [1–3].

The PMMW image sensor system can be applied to the field of the concealed-arm detection for the prevention of terror. After the 9.11 terror, all nations strengthen the security. It is expected to discern the terrorists in the public traffic or an airport by using small size and high sensitive PMMW.

Moreover, the PMMW image sensor can obtain an image due to the transparency of the wave regardless of the weather and can use in the aircraft landing in the bad weather. Besides, the PMMW image sensor can be very variously utilized in fields of the medical diagnosis such as the cancer cell detection, the fruit/vegetable culture and management, the nondestructive inspection, the environmental monitoring such as the observation of the red tide phenomenon, etc. So, the main purpose of this article is the development of W-band LNA MMIC, core component in 94-GHz PMMW by using a 0.1-μm InGaAs/InAlAs/GaAs mHEMT technology.

2. 0.1-μm InGaAs/InAlAs/GaAs mHEMT TECHNOLOGY

A GaAs-based low-noise mHEMT epitaxial structure with an In content of 53% in the InGaAs channel was grown by using molecular beam epitaxy. The cross-section of the mHEMT structure is shown in Figure 1. The mHEMT was grown on a 1-μm-thick graded buffer layer on a four-inch semi-insulating GaAs wafer, followed by a 300-nm-thick InAlAs buffer layer. We used a 20-nm-thick $In_{0.53}Ga_{0.47}As$ channel layer. The Si-planar doping layers were separated from the channel layer by thin 3-nm $In_{0.52}Al_{0.48}As$ undoped spacer layers, followed by a 12-nm-thick $In_{0.52}Al_{0.48}As$ undoped schottky layer and a 20-nm-thick $In_{0.53}Ga_{0.47}As$ cap layer doped with Si of 5×10^{18} cm^{-3} for obtaining a low ohmic resistance. The room temperature electron mobility (μ_H) of the mHEMT structure was found to be 9100 cm^2/V s, and the sheet carrier concentration (n_s) was found to be 3.2×10^{12} cm^{-2}.

Layers	Materials
Cap	InGaAs, 20 nm
Schottky	$In_{0.52}Al_{0.48}As$, 12 nm
Carrier supplier	Si, planar doped
Spacer	$In_{0.52}Al_{0.48}As$, 3 nm
Channel	$In_{0.53}Ga_{0.47}As$, 20 nm
Buffer	$In_{0.52}Al_{0.48}As$, 300 nm
Graded buffer	InAlAs, 1000 nm
Substrate	GaAs Substrate

Figure 1 Schematic cross-section of a low-noise mHEMT epitaxial structure